HHS Public Access

Author manuscript

Neuroimage. Author manuscript; available in PMC 2017 July 01.

Published in final edited form as:

Neuroimage. 2016 July 1; 134: 328–337. doi:10.1016/j.neuroimage.2016.03.070.

Structural Connectivity Relates to Perinatal Factors and Functional Impairment at 7 Years in Children Born Very Preterm

Deanne K. Thompson, PhD[a,b,c], **Jian Chen, ME**[a,d], **Richard Beare, PhD**[a,d], **Christopher L. Adamson, PhD**[a], **Rachel Ellis, PhD**[a], **Zohra M. Ahmadzai, BBiomed (hons)**[a], **Claire E. Kelly, BSc (hons)**[a], **Katherine J. Lee, PhD**[a,c], **Andrew Zalesky, PhD**[e,f], **Joseph Y.M. Yang, MBChB**[a,g], **Rodney W. Hunt, PhD**[a,c,h], **Jeanie L.Y. Cheong, MD**[a,i,j], **Terrie E. Inder, MBChB, MD**[k], **Lex W. Doyle, MD**[a,c,i,j], **Marc L. Seal, PhD**[a,c], and **Peter J. Anderson, PhD**[a,c]

[a]Murdoch Childrens Research Institute, 50 Flemington Road, Parkville, Victoria, 3052, Australia

[b]Florey Institute of Neuroscience and Mental Health, 30 Royal Parade, Parkville, Victoria, 3052, Australia

[c]Department of Paediatrics, University of Melbourne, 50 Flemington Road, Parkville, Victoria, 3052, Australia

[d]Department of Medicine, Monash Medical Centre, Monash University, 246 Clayton Rd, Melbourne, Victoria, 3168, Australia

[e]Department of Psychiatry, Melbourne Neuropsychiatry Centre, University of Melbourne and Melbourne Health, 161 Barry St, Carlton, Victoria, 3053, Australia

[f]Melbourne School of Engineering, Building 173, University of Melbourne, Parkville, Victoria, 3010, Australia

[g]Department of Neurosurgery, Royal Children's Hospital, 50 Flemington Road, Parkville, Victoria, 3052, Australia

[h]Department of Neonatal Medicine, The Royal Children's Hospital, 50 Flemington Road, Parkville, Victoria, 3052, Australia

[i]Women's Newborn Research Centre, Royal Women's Hospital, 20 Flemington Rd, Parkville, Victoria, 3052, Australia

[j]Department of Obstetrics and Gynaecology, University of Melbourne, 20 Flemington Rd, Parkville, Victoria, 3052, Australia

[k]Brigham and Women's Hospital, 75 Francis St, Boston, Massachusetts, 02115, United States

Abstract

Corresponding author: Deanne K. Thompson, Victorian Infant Brain Studies (VIBeS), Murdoch Childrens Research Institute, 50 Flemington Road, Parkville, Victoria, 3052, Australia, Phone +61 3 99366708, Fax +61 3 93481391, deanne.thompson@mcri.edu.au.

Objective—To use structural connectivity to (1) compare brain networks between typically and atypically developing (very preterm) children, (2) explore associations between potential perinatal developmental disturbances and brain networks, and (3) describe associations between brain networks and functional impairments in very preterm children.

Methods—26 full-term and 107 very preterm 7-year-old children (born <30 weeks' gestational age and/or <1250 g) underwent T_1- and diffusion-weighted imaging. Global white matter fiber networks were produced using 80 cortical and subcortical nodes, and edges created using constrained spherical deconvolution-based tractography. Global graph theory metrics were analysed, and regional networks were identified using network-based statistics. Cognitive and motor function were assessed at 7 years of age.

Results—Compared with full-term children, very preterm children had reduced density, lower global efficiency and higher local efficiency. Those with lower gestational age at birth, infection or higher neonatal brain abnormality score had reduced connectivity. Reduced connectivity within a widespread network was predictive of impaired IQ, while reduced connectivity within the right parietal and temporal lobes was associated with motor impairment in very preterm children.

Conclusions—This study utilized an innovative structural connectivity pipeline to reveal that children born very preterm have less connected and less complex brain networks compared with typically developing term-born children. Adverse perinatal factors led to disturbances in white matter connectivity, which in turn are associated with impaired functional outcomes, highlighting novel structure-function relationships.

Keywords

brain; diffusion weighted imaging; magnetic resonance imaging; preterm

Introduction

Graph theory is a sophisticated model for understanding complex networks. A graph consists of discrete objects ("nodes") and estimates of the degree of connectedness ("edges") between the objects. Graph theory has recently been applied to assess WM fiber networks (structural connectivity), allowing investigation of communication flow throughout the whole brain rather than isolated fiber tracts (Sporns et al., 2004). In the current study of structural connectivity, the "nodes" of the graph represent different brain regions, including both cortical and subcortical gray matter structures. The "edges" of the graph are the connecting WM fiber tracts (Bullmore and Sporns, 2012). Graph theory estimates of structural connectivity have been successfully applied to understand typical (Dennis et al., 2013; Hagmann et al., 2010) and atypical (Cao et al., 2013) brain development. In addition to global brain topology, connectomes (maps of WM connections in the brain) can be analysed for regional sub-network differences using network-based statistics (NBS) (Zalesky et al., 2010).

The very preterm (VP) population (<32 weeks' gestational age) provides a model to understand atypical connectome development, considering such infants are born during an important period involving rapidly developing neurobiological processes, including cell migration and white matter (WM) myelination (Volpe, 2008). This places VP infants at an

increased risk for brain injury compared with their full-term (FT) peers. The cerebral WM is particularly vulnerable to injury, which may be associated with, primary or secondary neuronal deafferentation (Volpe, 2009). Both neonatal brain injury and alterations in early and later brain development in VP children are associated with neurodevelopmental impairments in attention (Murray et al., 2014), memory (Omizzolo et al., 2014), language (Reidy et al., 2013), and motor functioning (Williams et al., 2010). The functional challenges that VP children face are likely due in part to altered WM connectivity and neural processing. While there has been much investigation into microstructural WM differences in isolated WM fiber tracts between VP and FT infants (Anderson et al., 2015; Pannek et al., 2014b), the investigation of large-scale global connectivity and regional differences in the connectome of VP children, and their relationship to perinatal factors and later outcomes is limited.

Previous studies in this field have used the diffusion tensor model to estimate local axonal orientations and obtain connectivity metrics, however this model has inherent limitations (Jones et al., 2013). In the current study, crossing fibers were explicitly modelled with constrained spherical deconvolution (Tournier et al., 2007). Furthermore, previous studies examining brain networks using structural connectivity have often neglected to include subcortical nodes, which are important relay stations in the brain (Hagmann et al., 2008), and are known to be particularly vulnerable to developmental disturbances such as prematurity (Boardman et al., 2006; Srinivasan et al., 2007). The structural connectivity pipeline utilized in the current study includes both cortical and subcortical nodes, and edges estimated using crossing fiber tractography, with constraints to exclude anatomically implausible tracts.

The current study will address unanswered questions about how cerebral WM networks differ during atypical development in VP compared with FT children, with the following aims: (1) To compare structural connectivity (both global measures and regional sub-networks within the connectome) between VP and FT children at 7 years of age; (2) To determine if structural connectivity is associated with perinatal factors that have been previously related to functional outcomes in the VP group; (3) To determine relationships between concurrent structural connectivity and functional impairments in VP children. We hypothesized that VP children would have developmentally delayed or disrupted brain connectivity (reduced density and global efficiency, higher local efficiency, and reduced connection strength within local sub-networks) compared with FT children, and that male sex, earlier gestational age at birth, lower birthweight standard deviation (SD) score and perinatal complications such as bronchopulmonary dysplasia, infection and brain abnormality would be associated with delayed or disrupted brain connectivity in VP children. We also hypothesized that reduced connection strength within regional brain sub-networks would be associated with functional impairments in VP children.

Materials and methods

Participants and scanning

224 VP (born at <30 weeks' gestational age and/or birthweight <1250 g) and 46 FT (born from 37 to 42 weeks' gestational age and ≥2500 g) infants were recruited during the

neonatal period into the Victorian Infant Brain Studies (VIBeS) cohort. Perinatal data were collected from chart review at the time of discharge on gestational age at birth, sex, birthweight SD score computed relative to the British Growth Reference data (Cole et al., 1998), bronchopulmonary dysplasia (oxygen dependency at 36 weeks' corrected age), infection (defined as one or more episodes of necrotising enterocolitis and/or culture positive sepsis) and total brain abnormality score based on magnetic resonance imaging (MRI) at term equivalent age (40 weeks ± 2 weeks) which was graded qualitatively (with a total possible score of 52), as previously described and validated (Kidokoro et al., 2013). At approximately 7 years of age, 198 VP and 43 FT children were followed up with neurodevelopmental assessments and MRI. Of those who were followed up, 160 VP and 36 FT children underwent MRI, but 63 of these either did not have complete diffusion or structural datasets acquired, or their scans were unusable primarily due to movement artifact. Thus, 49% (n= 133: 107 VP, 26 FT) of the original cohort had scans at age 7 years of sufficient quality for analysis in the current study. MRI was undertaken in unsedated participants in a Siemens 3T Magnetom Trio scanner at the Royal Children's Hospital, Melbourne. Children underwent 3-D T_1 weighted (0.85 mm sagittal slices, flip angle = 9°, repetition time = 1900 ms, echo time = 2.27 ms, field of view = 210 × 210 mm, matrix = 256 × 256) and single-shot twice-refocused echo-planar diffusion weighted imaging (45 gradient directions, b = 3000 s/mm^2, repetition time = 7600 ms; echo time = 110 ms; matrix = 104 × 104; field of view = 240 × 240 mm; voxel size = 2.3 mm isotropic).

Parental consent was obtained for all subjects, and ethics approval was obtained from the Royal Children's Hospital Human Research Ethics Committee prior to recruitment.

Magnetic Resonance Image analysis

WM connectivity graphs were constructed using segmentations of T_1 images into anatomical regions of interest, called nodes, with interconnecting WM fibers used to compute the edges.

Anatomical images were preprocessed by using Freesurfer to parcellate the cortex into 66 regions (Desikan et al., 2006) and 14 subcortical gray matter structures (Fischl et al., 2002), yielding graphs with N = 80 nodes. Whole intracranial volumes were also obtained using FreeSurfer. Individual subjects' node label images were then aligned with their corresponding diffusion weighted images using nonlinear registration with Advanced Normalisation Tools (ANTS) (Avants et al., 2008) following initial linear registration with the Functional MRI of the Brain Software Library's (FSL) linear registration tool (Jenkinson et al., 2002). This was achieved by initial registration of the non-diffusion weighted image to the T_1 image that had been intensity-inverted to better match the non-diffusion weighted image, followed by inversion of the non-linear warp field and affine matrix, enabling subsequent processing in diffusion space.

Diffusion images were preprocessed by performing eddy current and motion correction using a modified version of the 'eddy_correct' tool available in FSL. This modification restricts the mutual information-based registration cost function to brain voxels, by applying a weighting function. Therefore, the bias introduced by peripheral cerebrospinal fluid is minimized, thereby reducing excess scaling common for data acquired at b-values of 3000

s/mm^2 and higher (Adamson et al., 2013). The constrained spherical deconvolution model was used to represent the voxel-wise fiber orientation distribution estimates (Tournier et al., 2007), where the maximum harmonic order was chosen to be 6. MRtrix software was used to perform constrained spherical deconvolution-based probabilistic tractography with the FreeSurfer WM mask as the seed, and node masks as the endpoints (Tournier et al., 2012). Tractography parameters were: step size 1 mm, radius of curvature threshold 1.9 mm (maximum bending angle of 30° per mm). A common seeding voxel size was used for all subjects to ensure a consistent density of streamlines per mm^3 across subjects. Streamlines were seeded in the WM at a density of 2 streamlines per 0.7 mm^3. This resulted in dense coverage of the WM, enabling a close estimate of the underlying configuration of WM bundles based on the fiber orientation distributions. Streamlines were terminated if they left the combined gray and WM mask or reached the gray matter mask. This combination leads to termination on reaching cerebrospinal fluid, for example, and allows the ends of streamlines to lie *within* the gray matter mask but without allowing further propagation *through* it. Only streamlines with both ends in gray matter nodes contributed to graph edges, and those connecting the same node or with erroneous interhemispheric connections between deep gray nuclei were discarded.

Connectivity matrix generation

The connectivity matrix for each subject was denoted as: $W = [w_{ij}]$, $i, j \in 1 \ldots N$, $i \neq j$ where for each node pair (i, j) the undirected edge weights ($w_{ij} = w_{ji}$) were computed according to streamline count normalized by streamline length and average node volume (Hagmann et al., 2008), as follows:

$$w_{ij} = \frac{2}{V_i + V_j} \sum_h \frac{1}{l_h}$$

Where l_h denotes the arc length of streamline h, V_i and V_j denote the volume of the seeds i and j, respectively, and h cycles through all streamlines interconnecting nodes i and j. In order to remove connections deemed to arise from spurious streamlines, edges were discarded beginning at the weakest streamline count, until 1% of the total streamline count were discarded. The 1% of streamlines discarded does not represent the same number of edges in each subject, and therefore does not produce a uniform density across subjects.

Global Connectivity Measures

The global measures of connectivity employed were: raw density, global efficiency, local efficiency, and small-worldness. Raw density is a measure of gross connectedness, global efficiency is used as a measure of integration within the brain, local efficiency is a measure of clustering or segregation of brain regions and small-worldness is a measure of the balance between local efficiency (segregation) and global efficiency (integration), where a complex small-world topology consists of clusters of nodes connected via ‘hub’ nodes (Achard and Bullmore, 2007; Bullmore and Sporns, 2012).

Raw density was defined as the proportion of edges present to the number of edges in a completely dense graph, as follows:

$$\frac{1}{N(N-1)}\sum_{i\in 1\ldots N, j\in 1\ldots N} 1_{w_{ij}>0}$$

where $1_{w_{ij}>0}$ denotes an indicator function that equals 1 for $w_{ij}>0$ and zero otherwise.

The remaining measures (global efficiency, local efficiency, and small-worldness) are dependent on network density (van Wijk et al., 2010). Therefore, to avoid bias, edges were culled in order of increasing weight so that the top 30% of connections were retained for each subject. This maintained the highest density possible, while producing a uniform number of edges between subjects. In addition, these weight matrices were transformed into adjacency matrices denoted $A = [a_{ij}]$, where $a_{ij} = 1_{w_{ij}>0}$. All graph theory metrics were calculated using the unweighted adjacency matrix A.

Global efficiency was defined as (Achard and Bullmore, 2007):

$$E_{global}=\frac{1}{N(N-1)}\sum_{i\in 1\ldots N}\sum_{j\in 1\ldots N}\frac{1}{L_{ij}}$$

where L_{ij} denotes the shortest path length between nodes i and j on the adjacency matrix A.

Local efficiency was defined as (Achard and Bullmore, 2007):

$$E_{local}=\sum_{i\in 1\ldots N}\frac{\sum_{j\in 1\ldots N, h\in 1\ldots N, j\neq i} a_{ij}a_{ih}\left(L_{jh}(\mathcal{N}_i)\right)^{-1}}{k_i(k_i-1)}$$

where $L_{jh}(\mathcal{N}_i)$ denote the shortest path length between nodes j and h in the subgraph containing only the neighbours of node i.

Small-worldness, σ, was defined as the ratio of clustering coefficient, λ, to characteristic path length, γ, defined as (Watts and Strogatz, 1998):

$$\sigma=\frac{\lambda/\lambda_{rand}}{\gamma/\gamma_{rand}}$$

where λ_{rand}, γ_{rand}, denote characteristic path lengths and clustering coefficients from randomly generated networks of the same number of nodes and density. The characteristic path length was defined as the average of shortest path lengths for all node pairs as follows:

$$\lambda=\frac{1}{N(N-1)}\sum_{i\in 1\ldots N}\sum_{j\in 1\ldots N} L_{ij}$$

The clustering coefficient was defined as the mean of ratios of triangles to triples as follows:

$$\gamma = \frac{1}{N} \sum_{i \in 1 \ldots N} \frac{2 \sum_{j \in 1 \ldots N} \sum_{h \in 1 \ldots N} a_{ij} a_{ih} a_{jh}}{k_i (k_i - 1)}$$

where k_i denotes the degree of node i:

$$k_i = \sum_{j \in 1 \ldots N} a_{ij}$$

Graph metrics were computed using the python networkx package (http://networkx.github.io), and normalized metrics, such as small-worldness, were computed using randomized graphs which preserved degree distribution. Random graphs were generated using 5000 double-edge swaps, and 10 repeats.

Neurodevelopmental assessments

During the follow-up assessments at age 7 years, participants undertook an extensive battery of neurodevelopmental tests. Standardized scores were obtained for all assessments. The Wechsler Abbreviated Scale of Intelligence (WASI) was used to estimate general intelligence with a standardized mean of 100 and SD of 15 (Wechsler, 1999). Basic academic skills (word reading and math computation, mean= 100, SD= 15) were assessed using the Wide Range Achievement Test 4 (WRAT4) (Wilkinson and Robertson, 2005). Attention was assessed using the Score subtest (mean= 10, SD= 3) of the Test of Everyday Attention for Children (TEACh) (Manly et al., 1999). General language ability was measured using the Core Language scale (mean= 100, SD= 15) from the Clinical Evaluation of Language Fundamentals - 4th Edition Australian (CELF-IV) (Semel et al., 2006). Working memory was assessed using the Backward Digit Recall subtest (mean= 100, SD= 15) from the Working Memory Test Battery for Children (WMTB-C) (Pickering and Gathercole, 2001). Visual perceptual skills were estimated using the Visual Closure subtest (mean= 10, SD= 3) of the Test of Visual Perceptual Skills - 3rd Edition (TVPS-3) (Martin, 2006). Motor functioning was assessed using the Movement Assessment Battery for Children – version 2 (MABC2, mean= 10, SD= 3) (Henderson et al., 2007). Impairment variables were calculated for each outcome measure and used for all analyses, where impairment was defined as scoring more than 1 SD below the normative mean. The non-impaired comparison group were children who were not impaired on any of the above measures.

Statistical analyses

Statistical analyses were performed using Stata 13.1. Sample characteristics were compared between children included in the current study vs. those originally recruited but not included in this study separately for the VP and FT groups, and between FT and VP participants using means and SD, or numbers and percentages as appropriate.

For global network measures, group differences (VP vs. FT) and perinatal associations were assessed using separate linear regression models for each network measure, fitted using

generalized estimating equations and reported with robust standard errors to allow clustering of multiple births (i.e. allowing for the fact that multiple births are not independent). All estimates were adjusted for age at scan and intracranial volume. Group and the perinatal factors (gestational age at birth, sex, birthweight SD score, bronchopulmonary dysplasia, infection, and neonatal brain abnormality) were the independent predictor variables, while the network connectivity measure was the dependent or outcome variable. Perinatal predictors were assessed in the VP group only. The association between global connectivity measures and neurodevelopmental impairment was assessed using logistic regression, with impairment as the dependent variable and connectivity as the independent predictor variable, fitting separate regression models for each outcome-predictor combination. Again models were fitted using generalized estimating equations, and reported with robust standard errors to allow clustering of multiple births, and age at assessment and intracranial volume were included as covariates in the model.

Regional connectome analyses of group-wise differences (VP vs. FT), and associations between the connectome measures and perinatal factors and neurodevelopmental impairment within the VP group were conducted using NBS. Matched-density networks were thresholded at 50% so that common edges were present in at least 50% of subjects in the cohort, then NBS identified a set of connected components (sub-networks) that differed between groups or were associated with outcome, while correcting for Type 1 errors (false positives) using permutation testing. NBS first applied a statistical test to each edge in the complete network – e.g. a regression using edge weight as a predictor for an outcome measure or a t-test comparing edge weights between groups. A new graph was created using the test statistic as the edge weight, and edges below a specified threshold were removed. A range of t-statistic thresholds were tested (2.0 to 5.0 in increments of 0.25), and results from the threshold of 2.25 were presented, as this threshold tended to produce the most stable networks (evident over multiple thresholds). The “significance” of connected components in the resulting graph was estimated using permutation testing (n= 5000). For each permutation, subjects were randomly reallocated into a group, the test statistic was recalculated, and connected components were found. The size of the largest connected component was recorded for each permutation. If the cluster in the baseline test was larger than the largest cluster in 97% of the permutation tests, then it was considered significant at a family-wise error corrected level of 0.03. The effects of age at assessment and intracranial volume were controlled by including them as covariates in the regression at each edge. Due to multiple comparisons, all results were interpreted by identifying overall patterns and magnitudes of differences, rather than focusing on individual p-values, according to modern statistical practice (Kirkwood and Sterne, 2003).

Results

Sample characteristics

Demographics were generally similar between VP participants (n= 107) and non-participants (n= 117), except participants were less likely to be male (46% vs. 58%), exposed to postnatal corticosteroids (4% vs 15%), singleton (50% vs 66%), or diagnosed with intraventricular haemorrhage grade 3/4 (0.9% vs 6%). Characteristics were similar

between FT participants and non-participants. The proportion of males was similar between the VP and FT participants, but as expected gestational age at birth and birthweight SD score were lower and there were higher rates of all other perinatal variables for the VP group compared with FT group (Table 1). Brain abnormality scores ranged between 0 and 12 for the VP group and 0 and 5 for the FT group. The VP group had smaller intracranial volumes and higher rates of impairment on most neurodevelopmental measures at age 7 years compared with the FT group (Table 1).

Very preterm vs. full-term

The VP children had a lower density of connections [mean difference (95% confidence interval), *p*: −0.015 (−0.028, −0.001), 0.03], lower global efficiency [−0.002 (−0.003, −0.001), 0.001] and higher local efficiency [0.005 (0.002, 0.008), p=0.003] compared with FT children (Fig. 1). However, VP and FT children's brains had similar small-world properties [0.001 (−0.016, 0.019), 0.9]. NBS analyses did not find particular sub-networks that differed between VP and FT children (results not shown).

Perinatal predictors

Within the VP group, increasing gestational age at birth was associated with a higher density of connections, higher global efficiency, lower local efficiency and lower small-worldness (Fig 2). VP males had higher global efficiency than VP females. Infection was associated with lower density of connections within the whole brain of VP children. There was weak evidence for an association between neonatal brain abnormality and reduced density. There was little evidence that global connectivity measures in 7-year-old children were associated with birthweight SD score or bronchopulmonary dysplasia.

On NBS analysis, as brain abnormality score increased, there was reduced connection strength within a sub-network involving the left thalamus and putamen, the left inferior parietal cortex, and right cuneus, precuneus, pericalcarine and posterior cingulate cortex, and right supramarginal gyrus (p=0.042) (Fig 3A). The main hubs within this network component were the left thalamus, and the right supramarginal gyrus.

Infants with bronchopulmonary dysplasia had a trend toward reduced connection strength in 3 nodes on the left side (inferior temporal connected to both the lateral orbitofrontal and amygdala) (p=0.074) (Fig 3B).

There was some evidence that infants who had infection had reduced connection strength within a network component involving 9 nodes: bilateral caudal anterior cingulate cortex, pars opercularis and pars triangularis, as well as the left rostral middle frontal gyrus, and right caudal middle frontal gyrus and right caudate, but only at a lowered t-statistic threshold of 2.00 (p=0.0014) (Fig 3C). No clear network components were resolved that had differing connection strength between sexes or that were associated with gestational age at birth for the VP group on NBS analysis.

Neurodevelopmental impairment

There was little evidence for associations between global network measures and neurodevelopmental impairments in VP children at age 7 years (all p >0.05, data not shown). However, regional network analyses using NBS revealed that children with impaired IQ exhibited reduced connection strength in a diffuse network component consisting of 33 nodes, particularly on the right, compared with VP children without impairment (p=0.049). Nodes included the bilateral paracentral lobule, pars opercularis, posterior cingulate, and precuneus cortices, bilateral rostral middle frontal, superior frontal, and supramarginal gyri, and bilateral caudate regions, left pars orbitalis, and right banks of superior temporal sulcus, and pars triangularis, right cuneus, inferior parietal, lateral occipital, and superior parietal cortices, right caudal middle frontal, fusiform, inferior temporal, middle temporal, postcentral, precentral and superior temporal gyri, and right temporal pole, thalamus, and hippocampus (Fig 4A).

In contrast to VP children without impairment, VP children with impaired motor functioning displayed some evidence for reduced connection strength in a sub-network involving the right precuneus as the hub connected to the right inferior parietal, inferior temporal, middle temporal, and superior temporal gyri, at a raised t-statistic threshold of 3.0 (p=0.051) (Fig 4B). There were no network components associated with reading, mathematics, attention, language, visual perception or working memory impairments in VP children.

Discussion

This study reveals less complex brain connectivity in VP compared with typically developing term-born children, suggesting delay or disruption to brain development. Interestingly however, these *global* network differences did not appear to be associated with impaired functional outcomes in VP children. Rather, we discovered more targeted structure-function relationships, where differences in connectivity within particular *regional* sub-networks were associated with specific functional impairments in VP children. Furthermore, this study describes perinatal factors that predict white matter connectivity disturbances in VP children, including younger gestational age at birth, female sex, perinatal infection, and brain abnormality.

This study demonstrates that VP children have a less connected, less complex brain topology than FT children. The results indicate that the VP brain handles information efficiently within functional clusters, but overall the system is less efficient, requiring more steps to transfer information between distal brain regions than in FT children. These findings suggest that the VP brain has more segregated and less integrated networks than the FT brain at age 7 years, consistent with a less developed structural brain network. Other studies of healthy subjects have shown that increasing integration and decreasing segregation occur as the brain develops (Hagmann et al., 2010; Tymofiyeva et al., 2013). Such changes may be related to pruning and reinforcement of WM connections, i.e. the strengthening of long-range connections, but also the weakening of short-range connections (Hagmann et al., 2010). Our study is the first to demonstrate that there are differences in global structural connectivity metrics between VP and FT populations. However, we did not find regional sub-network differences in the connectome (on NBS) between groups at age 7 years.

Similarly, an *infant* connectome study by Ball *et al.* did not find differences between the preterm (<35 weeks' gestational age) and FT groups on the most highly connected set of cortical hubs (the 'rich club') (Ball et al., 2014). However, the same group demonstrated reduced thalamocortical connectivity in preterm compared with FT infants (Ball et al., 2013). Pannek et al. also performed a connectome study in a small group of infants using NBS, revealing a specific fronto-temporal cortical network that differed between groups (Pannek et al., 2013). Differences between these infant findings and the current findings in 7 year-olds may be due to compensatory mechanisms during early childhood, or population and methodological differences between studies, as both previous infant studies used anisotropy to weight edges rather than normalized probabilistic streamline count. Alternatively, our finding of altered global structural connectivity in VP vs. FT children may suggest that the VP brain has more widespread immaturity, rather than specifically vulnerable regions. This is consistent with our previous findings where there were no specific regional vulnerabilities for VP compared with FT infants when assessing eight WM regions per hemisphere using diffusion tensor imaging (Thompson et al., 2014). Previous studies of WM structure have tended to focus on individual WM regions using methods such as tractography or regions of interest. These previous studies have shown that VP children have altered microstructure in specific tracts such as the corpus callosum, corticospinal tracts or optic radiations, which often correlate with neurodevelopmental delays (Pannek et al., 2014b; Thompson et al., 2015). However, in contrast to previous regional studies, the graph theory method used in the current study enabled us to provide novel evidence that the complexity of the whole brain connectome is altered in VP children.

VP children born at a younger gestational age had a lower density of connections, poorer integration and higher segregation, with higher small-worldness, consistent with delayed or disrupted development (Dennis et al., 2013; Hagmann et al., 2010; Tymofiyeva et al., 2013). In agreement with our findings, lower gestational age has previously been associated with poorer integration and higher segregation, when comparing moderately preterm with extremely preterm 6 year old children (Fischi-Gomez et al., 2014).

Neonatal brain abnormality was associated with persistent disruption to structural connectivity or alterations to WM 'wiring' over the first 7 years of life. This highlights the important prognostic power of neonatal MRI, as previously suggested (Woodward et al., 2006). Brain regions with reduced connection strength in the presence of neonatal brain abnormality included the left thalamus and right supramarginal gyrus as the main hubs, and the left putamen and regions within the occipital and parietal lobe (including right precuneus). A reduction in the streamline count in the network comprising those with neonatal brain abnormality might reflect white matter pathology owing to altered axonal packing density, myelination or axonal diameter. Both intra- and inter-hemispheric connections were involved. It is well known that neonatal brain injury in preterm infants, such as periventricular leukomalacia, affects many parts of the brain including the corpus callosum (Thompson et al., 2012), thalamus and cortex (Volpe, 2009). Our study provides further support for the vulnerability of the corpus callosum and thalamocortical connections to neonatal brain injury in VP children. Altered thalamocortical connectivity has previously been reported in preterm infants, however notably infants in that study did not have any overt brain injury (Ball et al., 2013).

This study found evidence for a relationship between perinatal infection and a lower density of white matter connections in VP children. This is the first study to report a relationship between perinatal infection and structural connectivity in VP children, however previous studies have shown associations between infection and other brain abnormalities (Strunk et al., 2014; Volpe, 2009) or WM microstructural alterations (Chau et al., 2012) in preterm infants. An interhemispheric frontal sub-network may have been particularly affected. The underlying WM tract in this sub-network is likely to be the genu of the corpus callosum, which connects frontal regions interhemispherically. We have previously shown that the genu of the corpus callosum is compromized in VP infants on diffusion MRI (Thompson et al., 2011). Furthermore, associations between infection and lower fractional anisotropy in the genu of preterm infants have also been reported (Chau et al., 2012), in line with our current study.

VP males appeared to have a more integrated brain network than VP females. This is an unexpected finding considering males are generally reported to have more brain abnormalities and poorer neurodevelopmental and behavioural outcomes following prematurity than females (Ment and Vohr, 2008). Other studies examining graph theory metrics have shown that in general, healthy female adults have higher global and local efficiency relative to brain size (Gong et al., 2009b). Our study, however, is the first to reveal that the normal sexual asymmetry in structural connectivity is altered in VP children, suggesting sex-specific atypical development. An alternative explanation is that these findings may reflect a compensatory effect in VP males. These findings warrant clarification from future studies.

Bronchopulmonary dysplasia was associated with reduced connection strength within a sub-network connecting the inferior temporal gyrus to both the amygdala and lateral orbitofrontal cortex in the left hemisphere. The inferior longitudinal fasciculus is known to connect the inferior temporal and amygdala regions (Catani et al., 2003; Kier et al., 2004). The connection between the inferior temporal gyrus and lateral orbitofrontal cortex is likely to be directly via the inferior fronto-occipital fasciculus (Martino et al., 2010) or indirectly via multiple WM fiber tracts. The regions represented in the sub-network incorporate the anatomical temporal stem, consisting of multiple crossing-fiber populations from the inferior longitudinal fasciculus, the inferior fronto-occipital fasciculus, the uncinate fasciculus, and the optic radiation (Kier et al., 2004; Martino et al., 2010; Thiebaut de Schotten et al., 2012). Disentangling the connectivity contribution from each WM fiber population is not possible at the diffusion MRI voxel resolution used in this study. It has long been known that lung disease affects WM microstructure in preterm infants (Ball et al., 2010). However, to date no study has found an association between bronchopulmonary dysplasia and structural connectivity in childhood.

Despite our hypothesis that poorer intrauterine growth would be associated with altered brain networks (Rees et al., 2011), we did not find evidence of a relationship between birthweight SD score and structural connectivity within global or regional brain networks. In contrast, other studies have shown that intrauterine growth restriction was associated with poorer structural connectivity in one year old infants (Batalle et al., 2012) and 6 year olds (Fischi-Gomez et al., 2014), which also contributed to poorer neurodevelopmental

outcomes. This may reflect inherent perinatal differences in the cohorts reported and further research is warranted.

The current study is the first to report an association between a brain sub-network and IQ in VP children. This network component was made up of a diffuse set of regions with reduced connection strengths, including parts of the orbitofrontal and frontal cortices, cingulate cortex, parietal, temporal, and occipital lobes, and thalami and hippocampi. Many of these regions connected interhemispherically, implicating the corpus callosum as a contributing WM pathway, but thalamocortical and other major tracts may also have been involved. In agreement with our results, both the corpus callosum (Caldu et al., 2006) and thalamus (Zubiaurre-Elorza et al., 2012) have previously been associated with IQ or cognition in preterm populations, as have a range of other WM tracts (Feldman et al., 2012), and the hippocampus (Isaacs et al., 2004). Similar to the current study, structural connectivity within the cortico-basal ganglia-thalamo-cortical circuit, as well as short cortico-cortical connections, has been associated with higher order cognitive and social skills in extremely preterm children (Fischi-Gomez et al., 2014). In the current study, poorer connectivity in the right side of the brain appeared particularly associated with impaired IQ. The right hemisphere generally has more important hub regions, as evidenced by a higher betweenness centrality metric in healthy young adults (Gong et al., 2009a), and therefore the structural maturity of this hemisphere may be more indispensable for cognitive functioning in VP children. We have previously shown that microstructure of the right hemisphere WM is more vulnerable than the left in this cohort in infancy (Thompson et al., 2014), and the current study may reflect a cognitive consequence of this at 7 years of age.

This study found some evidence that motor impairment may be associated with reduced connectivity in a sub-network involving a right precuneus hub connecting to another right parietal region (inferior parietal) and the right temporal lobe (inferior, middle and superior). The precuneus has both anatomical cortico-subcortical and cortico-cortical connections, including to the inferior parietal and superior temporal regions (Cavanna and Trimble, 2006), is known to be an important hub from both structural and functional connectivity studies, and is implicated in the default mode network (Gong et al., 2009a). Although precuneus connections are thought to mediate mainly visuo-spatial imagery, episodic memory retrieval and self-processing operations, precuneus connections with the premotor and supplementary motor regions are involved in oculomotor functioning and visual guidance of movements (Cavanna and Trimble, 2006). Such connections may be the basis for the link we found between this precuneus sub-network and motor impairment in VP children. The cingulum bundle has projections to the precuneus and is known to be involved in motor control (Shima et al., 1991), and is therefore a possible underlying WM tract in this sub-network. The associations between motor impairment and a right sided sub-network in VP children may relate to known functional asymmetries in preterm populations, reflected by almost double the rate of non-right handedness compared with FT populations (Domellof et al., 2011). Furthermore, graph theory brain connectivity metrics have revealed hemispheric asymmetries during normal development (Dennis et al., 2013), which may explain the functional vulnerability of the right side in atypically developing VP children. The only study to date using NBS connectomics to find neural correlates of motor impairment in children was by Pannek et al., who reported associations between bimanual

tasks in children with cerebral palsy and fractional anisotropy within the cortico-spinal and thalamo-cortical pathways (Pannek et al., 2014a). However, many previous studies have used other diffusion imaging techniques to associate altered microstructure of the corona radiata, posterior limb of the internal capsule, corpus callosum and corticospinal tracts with motor functioning in preterm populations (de Kieviet et al., 2014; Kaukola et al., 2010; Rose et al., 2007; Thompson et al., 2012).

A common limitation associated with paediatric cohorts is motion artifact due to head movement, which may bias results toward more short-range rather than long-range connections (Satterthwaite et al., 2013), and could possibly affect the calculation of local efficiency. The accuracy of connectivity measures relies on precise white matter fiber tractography, which is affected by a range of factors, beginning with the diffusion image acquisition. Repetition and echo time, voxel size, gradient distribution and number of directions, and particularly *b*-value, all affect connectivity analyses (Xie et al., 2015). At the time of acquisition our sequence was optimized for constrained spherical deconvolution, however recent advances mean imaging acquisition can be improved even further for future connectivity studies. Furthermore, although our twice-refocused echo planar acquisition minimized image distortion due to eddy currents, future studies would benefit from acquisition and application of phase reversal images to more accurately correct for echo planar image susceptibility-induced distortion (Gallichan et al., 2010). Post-acquisition processing techniques are also evolving rapidly, and superior techniques are now available to correct for biases in streamline count (Smith et al., 2015), and to weight streamlines based on higher order models of diffusion (Raffelt et al., 2012), which would benefit future studies. In this study, non-linear image registration was used to align diffusion and structural images. Although label boundaries appeared to be satisfactorily aligned, any residual misalignment may influence subsequent connectivity metrics. We were also limited by the small sample size of the FT group, which lowered statistical power. There were very few functionally impaired FT children, and therefore investigation of associations between structural connectivity and functional outcomes in the normative FT 7-year-old population was not possible. Even within our VP group, the evidence for some of the NBS associations with perinatal factors and functional outcomes was weak. Further research is required to confirm our findings and to determine whether structural connectivity of VP children catches up into adolescence, as it has been shown that structure-function correlations increase with age (Hagmann et al., 2010), and network characteristics continue to change over adolescence and early adulthood (Dennis et al., 2013; Vertes and Bullmore, 2014).

In conclusion, this study utilized an innovative structural connectivity pipeline to reveal that adverse perinatal events can adversely affect brain connectivity 7 years later. Findings indicated that VP birth is associated with atypical development, disturbing brain connectivity, complexity and network structure 7 years later, as revealed by these children having less integrated and more segregated brains than FT 7 year olds. In particular, this study highlights the potential causes for the developmental vulnerability of VP children. Specific perinatal factors affecting the brain in the VP group were younger gestational age at birth, female sex, perinatal infection, and brain abnormality, all of which were associated with poorer connection strength. This implies that perinatal events have a lasting impact on WM connectivity in the brain at 7 years of age. Importantly, we also showed that poorer

connection strength in certain brain sub-networks was associated with impairments in IQ within VP children. This study suggests that structural connectivity analysis may be useful for identifying VP children at risk of neurodevelopmental impairment, enabling investigation of large-scale brain networks rather than isolated WM fiber tracts.

Acknowledgments

Funding

This work was supported by Australia's National Health and Medical Research Council (Centre for Clinical Research Excellence 546519 to LD, PA, TI, RH and JLYC; Centre for Research Excellence 1060733 to LD, PA, RH, JLYC and DT; Project grants 237117 to LD, 491209 to PA; Senior Research Fellowship 1081288 to PA; Career Development Fellowship 1085754 to DT; Early Career Fellowships 1012236 to DT, 1053787 to JLYC; Postgraduate Scholarship 1039160 to JY), National Institutes of Health (HD058056), United Cerebral Palsy Foundation (USA), Leila Y. Mathers Charitable Foundation (USA), the Brown Foundation (USA), the Victorian Government's Operational Infrastructure Support Program, and The Royal Children's Hospital Foundation (RCH1000 to JY).

We gratefully thank Merilyn Bear for recruitment, Michael Kean and the radiographers at Melbourne Children's MRI Centre, the VIBeS and Developmental Imaging groups at the Murdoch Childrens Research Institute for their ideas and support, as well as the families and children who participated in this study.

References

Achard S, Bullmore E. Efficiency and cost of economical brain functional networks. PLoS Comput Biol. 2007; 3:174–183.

Adamson, CL.; Beare, R.; Thompson, DK.; Seal, M. Improved Accuracy of Motion and Affine Eddy Current Distortion Correction in High B-Value Diffusion Weighted Imaging Using Brain Mask Based Weighting Functions. International Society for Magnetic Resonance in Medicine 21st Annual Meeting & Exhibition; Salt Lake City, Utah, USA. 2013.

Anderson PJ, Cheong JL, Thompson DK. The predictive validity of neonatal MRI for neurodevelopmental outcome in very preterm children. Semin Perinatol. 2015

Avants BB, Epstein CL, Grossman M, Gee JC. Symmetric diffeomorphic image registration with cross-correlation: evaluating automated labeling of elderly and neurodegenerative brain. Med Image Anal. 2008; 12:26–41. [PubMed: 17659998]

Ball G, Aljabar P, Zebari S, Tusor N, Arichi T, Merchant N, Robinson EC, Ogundipe E, Rueckert D, Edwards AD, Counsell SJ. Rich-club organization of the newborn human brain. Proc Natl Acad Sci U S A. 2014; 111:7456–7461. [PubMed: 24799693]

Ball G, Boardman JP, Aljabar P, Pandit A, Arichi T, Merchant N, Rueckert D, Edwards AD, Counsell SJ. The influence of preterm birth on the developing thalamocortical connectome. Cortex. 2013; 49:1711–1721. [PubMed: 22959979]

Ball G, Counsell SJ, Anjari M, Merchant N, Arichi T, Doria V, Rutherford MA, Edwards AD, Rueckert D, Boardman JP. An optimised tract-based spatial statistics protocol for neonates: Applications to prematurity and chronic lung disease. NeuroImage. 2010; 53:94–102. [PubMed: 20510375]

Batalle D, Eixarch E, Figueras F, Munoz-Moreno E, Bargallo N, Illa M, Acosta-Rojas R, Amat-Roldan I, Gratacos E. Altered small-world topology of structural brain networks in infants with intrauterine growth restriction and its association with later neurodevelopmental outcome. NeuroImage. 2012; 60:1352–1366. [PubMed: 22281673]

Boardman JP, Counsell SJ, Rueckert D, Kapellou O, Bhatia KK, Aljabar P, Hajnal J, Allsop JM, Rutherford MA, Edwards AD. Abnormal deep grey matter development following preterm birth detected using deformation-based morphometry. NeuroImage. 2006; 32:70–78. [PubMed: 16675269]

Bullmore E, Sporns O. The economy of brain network organization. Nat Rev Neurosci. 2012; 13:336–349. [PubMed: 22498897]

Caldu X, Narberhaus A, Junque C, Gimenez M, Vendrell P, Bargallo N, Segarra D, Botet F. Corpus callosum size and neuropsychologic impairment in adolescents who were born preterm. J Child Neurol. 2006; 21:406–410. [PubMed: 16901446]

Cao Q, Shu N, An L, Wang P, Sun L, Xia MR, Wang JH, Gong GL, Zang YF, Wang YF, He Y. Probabilistic diffusion tractography and graph theory analysis reveal abnormal white matter structural connectivity networks in drug-naive boys with attention deficit/hyperactivity disorder. J Neurosci. 2013; 33:10676–10687. [PubMed: 23804091]

Catani M, Jones DK, Donato R, Ffytche DH. Occipito-temporal connections in the human brain. Brain. 2003; 126:2093–2107. [PubMed: 12821517]

Cavanna AE, Trimble MR. The precuneus: a review of its functional anatomy and behavioural correlates. Brain. 2006; 129:564–583. [PubMed: 16399806]

Chau V, Brant R, Poskitt KJ, Tam EW, Synnes A, Miller SP. Postnatal infection is associated with widespread abnormalities of brain development in premature newborns. Pediatr Res. 2012; 71:274–279. [PubMed: 22278180]

Cole TJ, Freeman JV, Preece MA. British 1990 growth reference centiles for weight, height, body mass index and head circumference fitted by maximum penalized likelihood. Stat Med. 1998; 17:407–429. [PubMed: 9496720]

de Kieviet JF, Pouwels PJ, Lafeber HN, Vermeulen RJ, van Elburg RM, Oosterlaan J. A crucial role of altered fractional anisotropy in motor problems of very preterm children. Eur J Paediatr Neurol. 2014; 18:126–133. [PubMed: 24119780]

Dennis EL, Jahanshad N, McMahon KL, de Zubicaray GI, Martin NG, Hickie IB, Toga AW, Wright MJ, Thompson PM. Development of brain structural connectivity between ages 12 and 30: A 4-Tesla diffusion imaging study in 439 adolescents and adults. NeuroImage. 2013; 64:671–684. [PubMed: 22982357]

Desikan RS, Segonne F, Fischl B, Quinn BT, Dickerson BC, Blacker D, Buckner RL, Dale AM, Maguire RP, Hyman BT, Albert MS, Killiany RJ. An automated labeling system for subdividing the human cerebral cortex on MRI scans into gyral based regions of interest. NeuroImage. 2006; 31:968–980. [PubMed: 16530430]

Domellof E, Johansson AM, Ronnqvist L. Handedness in preterm born children: a systematic review and a meta-analysis. Neuropsychologia. 2011; 49:2299–2310. [PubMed: 21601584]

Feldman HM, Lee ES, Loe IM, Yeom KW, Grill-Spector K, Luna B. White matter microstructure on diffusion tensor imaging is associated with conventional magnetic resonance imaging findings and cognitive function in adolescents born preterm. Dev Med Child Neurol. 2012; 54:809–814. [PubMed: 22803787]

Fischi-Gomez E, Vasung L, Meskaldji DE, Lazeyras F, Borradori-Tolsa C, Hagmann P, Barisnikov K, Thiran JP, Huppi PS. Structural Brain Connectivity in School-Age Preterm Infants Provides Evidence for Impaired Networks Relevant for Higher Order Cognitive Skills and Social Cognition. Cereb Cortex. 2014

Fischl B, Salat DH, Busa E, Albert M, Dieterich M, Haselgrove C, van der Kouwe A, Killiany R, Kennedy D, Klaveness S, Montillo A, Makris N, Rosen B, Dale AM. Whole brain segmentation: automated labeling of neuroanatomical structures in the human brain. Neuron. 2002; 33:341–355. [PubMed: 11832223]

Gallichan D, Andersson JL, Jenkinson M, Robson MD, Miller KL. Reducing distortions in diffusion-weighted echo planar imaging with a dual-echo blip-reversed sequence. Magn Reson Med. 2010; 64:382–390. [PubMed: 20665782]

Gong G, He Y, Concha L, Lebel C, Gross DW, Evans AC, Beaulieu C. Mapping Anatomical Connectivity Patterns of Human Cerebral Cortex Using In Vivo Diffusion Tensor Imaging Tractography. Cereb Cortex. 2009a; 19:524–536. [PubMed: 18567609]

Gong G, Rosa-Neto P, Carbonell F, Chen ZJ, He Y, Evans AC. Age- and Gender-Related Differences in the Cortical Anatomical Network. J Neurosci. 2009b; 29:15684–15693. [PubMed: 20016083]

Hagmann P, Cammoun L, Gigandet X, Meuli R, Honey CJ, Wedeen VJ, Sporns O. Mapping the structural core of human cerebral cortex. PLoS Biol. 2008; 6:1479–1493.

Hagmann P, Sporns O, Madan N, Cammoun L, Pienaar R, Wedeen VJ, Meuli R, Thiran JP, Grant PE. White matter maturation reshapes structural connectivity in the late developing human brain. Proc Natl Acad Sci U S A. 2010; 107:19067–19072. [PubMed: 20956328]

Henderson, SE.; Sudgen, DA.; Barnett, AL. Movement Assessment Battery for Children - Second Edition (Movement ABC-2). The Psychological Corporation; London (UK): 2007.

Isaacs EB, Edmonds CJ, Chong WK, Lucas A, Morley R, Gadian DG. Brain morphometry and IQ measurements in preterm children. Brain. 2004; 127:2595–2607. [PubMed: 15371289]

Jenkinson M, Bannister P, Brady M, Smith S. Improved optimization for the robust and accurate linear registration and motion correction of brain images. NeuroImage. 2002; 17:825–841. [PubMed: 12377157]

Jones DK, Knosche TR, Turner R. White matter integrity, fiber count, and other fallacies: the do's and don'ts of diffusion MRI. NeuroImage. 2013; 73:239–254. [PubMed: 22846632]

Kaukola T, Perhomaa M, Vainionpaa L, Tolonen U, Jauhiainen J, Paakko E, Hallman M. Apparent Diffusion Coefficient on Magnetic Resonance Imaging in Pons and in Corona Radiata and Relation with the Neurophysiologic Measurement and the Outcome in Very Preterm Infants. Neonatology. 2010; 97:15–21. [PubMed: 19571583]

Kidokoro H, Neil JJ, Inder TE. New MR imaging assessment tool to define brain abnormalities in very preterm infants at term. Am J Neuroradiol. 2013; 34:2208–2214. [PubMed: 23620070]

Kier EL, Staib LH, Davis LM, Bronen RA. MR imaging of the temporal stem: anatomic dissection tractography of the uncinate fasciculus, inferior occipitofrontal fasciculus, and Meyer's loop of the optic radiation. AJNR Am J Neuroradiol. 2004; 25:677–691. [PubMed: 15140705]

Kirkwood, BR.; Sterne, JAC. Medical Statistics. 2. Blackwell Publishing; Massachusetts (USA): 2003.

Manly, T.; Robertson, IH.; Anderson, V.; Nimmo-Smith, I. TEA-Ch: The Test of Everyday Attention for Children. Thames Valley Test Company; Bury St. Edmunds (England): 1999.

Martin, N. Test of Visual Perceptual Skills. 3. Academic Therapy Publications; Novato, California: 2006. TVPS-3

Martino J, Vergani F, Robles SG, Duffau H. New insights into the anatomic dissection of the temporal stem with special emphasis on the inferior fronto-occipital fasciculus: implications in surgical approach to left mesiotemporal and temporoinsular structures. Neurosurgery. 2010; 66:4–12. [PubMed: 20173571]

Ment LR, Vohr BR. Preterm birth and the developing brain. Lancet Neurol. 2008; 7:378–379. [PubMed: 18420149]

Murray AL, Scratch SE, Thompson DK, Inder TE, Doyle LW, Anderson JF, Anderson PJ. Neonatal brain pathology predicts adverse attention and processing speed outcomes in very preterm and/or very low birth weight children. Neuropsychology. 2014; 28:552–562. [PubMed: 24708047]

Omizzolo C, Scratch SE, Stargatt R, Kidokoro H, Thompson DK, Lee KJ, Cheong J, Neil J, Inder TE, Doyle LW, Anderson PJ. Neonatal brain abnormalities and memory and learning outcomes at 7 years in children born very preterm. Memory. 2014; 22:605–615. [PubMed: 23805915]

Pannek K, Boyd RN, Fiori S, Guzzetta A, Rose SE. Assessment of the structural brain network reveals altered connectivity in children with unilateral cerebral palsy due to periventricular white matter lesions. Neuroimage Clin. 2014a; 5:84–92. [PubMed: 25003031]

Pannek K, Hatzigeorgiou X, Colditz PB, Rose S. Assessment of structural connectivity in the preterm brain at term equivalent age using diffusion MRI and T2 relaxometry: a network-based analysis. PLoS One. 2013; 8:e68593. [PubMed: 23950872]

Pannek K, Scheck SM, Colditz PB, Boyd RN, Rose SE. Magnetic resonance diffusion tractography of the preterm infant brain: a systematic review. Dev Med Child Neurol. 2014b; 56:113–124. [PubMed: 24102176]

Pickering, S.; Gathercole, S. Working Memory Test Battery for Children - Manual. The Psychological Corporation; London (England): 2001.

Raffelt D, Tournier JD, Rose S, Ridgway GR, Henderson R, Crozier S, Salvado O, Connelly A. Apparent Fibre Density: a novel measure for the analysis of diffusion-weighted magnetic resonance images. NeuroImage. 2012; 59:3976–3994. [PubMed: 22036682]

Rees S, Harding R, Walker D. The biological basis of injury and neuroprotection in the fetal and neonatal brain. Int J Dev Neurosci. 2011; 29:551–563. [PubMed: 21527338]

Reidy N, Morgan A, Thompson DK, Inder TE, Doyle LW, Anderson PJ. Impaired language abilities and white matter abnormalities in children born very preterm and/or very low birth weight. J Pediatr. 2013; 162:719–724. [PubMed: 23158026]

Rose J, Mirmiran M, Butler EE, Lin CY, Barnes PD, Kermoian R, Stevenson DK. Neonatal microstructural development of the internal capsule on diffusion tensor imaging correlates with severity of gait and motor deficits. Dev Med Child Neurol. 2007; 49:745–750. [PubMed: 17880643]

Satterthwaite TD, Elliott MA, Gerraty RT, Ruparel K, Loughead J, Calkins ME, Eickhoff SB, Hakonarson H, Gur RC, Gur RE, Wolf DH. An improved framework for confound regression and filtering for control of motion artifact in the preprocessing of resting-state functional connectivity data. NeuroImage. 2013; 64:240–256. [PubMed: 22926292]

Semel, E.; Wiig, E.; Secord, W. Clinical Evaluation of Language Fundamentals- Fourth Edition, Australian Standardised Edition (CELF-4 Australian). Harcourt Assessment; Marrickville (Australia): 2006.

Shima K, Aya K, Mushiake H, Inase M, Aizawa H, Tanji J. Two movement-related foci in the primate cingulate cortex observed in signal-triggered and self-paced forelimb movements. J Neurophysiol. 1991; 65:188–202. [PubMed: 2016637]

Smith RE, Tournier JD, Calamante F, Connelly A. SIFT2: Enabling dense quantitative assessment of brain white matter connectivity using streamlines tractography. NeuroImage. 2015; 119:338–351. [PubMed: 26163802]

Sporns O, Chialvo DR, Kaiser M, Hilgetag CC. Organization, development and function of complex brain networks. Trends Cogn Sci. 2004; 8:418–425. [PubMed: 15350243]

Srinivasan L, Dutta R, Counsell SJ, Allsop JM, Boardman JP, Rutherford MA, Edwards AD. Quantification of deep gray matter in preterm infants at term-equivalent age using manual volumetry of 3-tesla magnetic resonance images. Pediatrics. 2007; 119:759–765. [PubMed: 17403847]

Strunk T, Inder T, Wang X, Burgner D, Mallard C, Levy O. Infection-induced inflammation and cerebral injury in preterm infants. Lancet Infect Dis. 2014; 14:751–762. [PubMed: 24877996]

Thiebaut de Schotten M, Dell'Acqua F, Valabregue R, Catani M. Monkey to human comparative anatomy of the frontal lobe association tracts. Cortex. 2012; 48:82–96. [PubMed: 22088488]

Thompson DK, Inder TE, Faggian N, Johnston L, Warfield SK, Anderson PJ, Doyle LW, Egan GF. Characterization of the corpus callosum in very preterm and full-term infants utilizing MRI. NeuroImage. 2011; 55:479–490. [PubMed: 21168519]

Thompson DK, Inder TE, Faggian N, Warfield SK, Anderson PJ, Doyle LW, Egan GF. Corpus callosum alterations in very preterm infants: perinatal correlates and 2 year neurodevelopmental outcomes. NeuroImage. 2012; 59:3571–3581. [PubMed: 22154956]

Thompson DK, Lee KJ, Egan GF, Warfield SK, Doyle LW, Anderson PJ, Inder TE. Regional white matter microstructure in very preterm infants: predictors and 7 year outcomes. Cortex. 2014; 52:60–74. [PubMed: 24405815]

Thompson DK, Lee KJ, van Bijnen L, Leemans A, Pascoe L, Scratch SE, Cheong J, Egan GF, Inder TE, Doyle LW, Anderson PJ. Accelerated corpus callosum development in prematurity predicts improved outcome. Hum Brain Mapp. 2015; 36:3733–3748. [PubMed: 26108187]

Tournier JD, Calamante F, Connelly A. Robust determination of the fibre orientation distribution in diffusion MRI: non-negativity constrained super-resolved spherical deconvolution. NeuroImage. 2007; 35:1459–1472. [PubMed: 17379540]

Tournier JD, Calamante F, Connelly A. MRtrix: Diffusion tractography in crossing fiber regions. International Journal of Imaging Systems and Technology. 2012; 22:53–66.

Tymofiyeva O, Hess CP, Ziv E, Lee PN, Glass HC, Ferriero DM, Barkovich AJ, Xu D. A DTI-based template-free cortical connectome study of brain maturation. PLoS One. 2013; 8:e63310. [PubMed: 23675475]

van Wijk BC, Stam CJ, Daffertshofer A. Comparing brain networks of different size and connectivity density using graph theory. PLoS One. 2010; 5:e13701. [PubMed: 21060892]

Vertes PE, Bullmore ET. Annual Research Review: Growth connectomics - the organization and reorganization of brain networks during normal and abnormal development. J Child Psychol Psychiatry. 2014; 56:299–320. [PubMed: 25441756]

Volpe, JJ. Neurology of the newborn. 5. Saunders Elsevier; Philadelphia: 2008.

Volpe JJ. Brain injury in premature infants: a complex amalgam of destructive and developmental disturbances. Lancet Neurol. 2009; 8:110–124. [PubMed: 19081519]

Watts DJ, Strogatz SH. Collective dynamics of 'small-world' networks. Nature. 1998; 393:440–442. [PubMed: 9623998]

Wechsler, D. Wechsler Abbreviated Scale of Intelligence (WASI). The Psychological Corporation; 1999.

Wilkinson, GS.; Robertson, GJ. Wide Range Achievement Test. 4. Wilmington: Delaware; 2005.

Williams J, Lee KJ, Anderson PJ. Prevalence of motor-skill impairment in preterm children who do not develop cerebral palsy: a systematic review. Dev Med Child Neurol. 2010; 52:232–237. [PubMed: 20002114]

Woodward LJ, Anderson PJ, Austin NC, Howard K, Inder TE. Neonatal MRI to predict neurodevelopmental outcomes in preterm infants. N Engl J Med. 2006; 355:685–694. [PubMed: 16914704]

Xie S, Zuo N, Shang L, Song M, Fan L, Jiang T. How does B-value affect HARDI reconstruction using clinical diffusion MRI data? PLoS One. 2015; 10:e0120773. [PubMed: 25803023]

Zalesky A, Fornito A, Bullmore ET. Network-based statistic: Identifying differences in brain networks. NeuroImage. 2010; 53:1197–1207. [PubMed: 20600983]

Zubiaurre-Elorza L, Soria-Pastor S, Junque C, Fernandez-Espejo D, Segarra D, Bargallo N, Romano-Berindoague C, Macaya A. Thalamic changes in a preterm sample with periventricular leukomalacia: correlation with white-matter integrity and cognitive outcome at school age. Pediatr Res. 2012; 71:354–360. [PubMed: 22391635]

Highlights

- Brain connectivity is less complex in very preterm than full-term children
- Brain networks in childhood are negatively impacted by adverse perinatal events
- Altered brain sub-networks are associated with impaired intelligence and movement
- We reveal causes and consequences for developmental vulnerability of the connectome

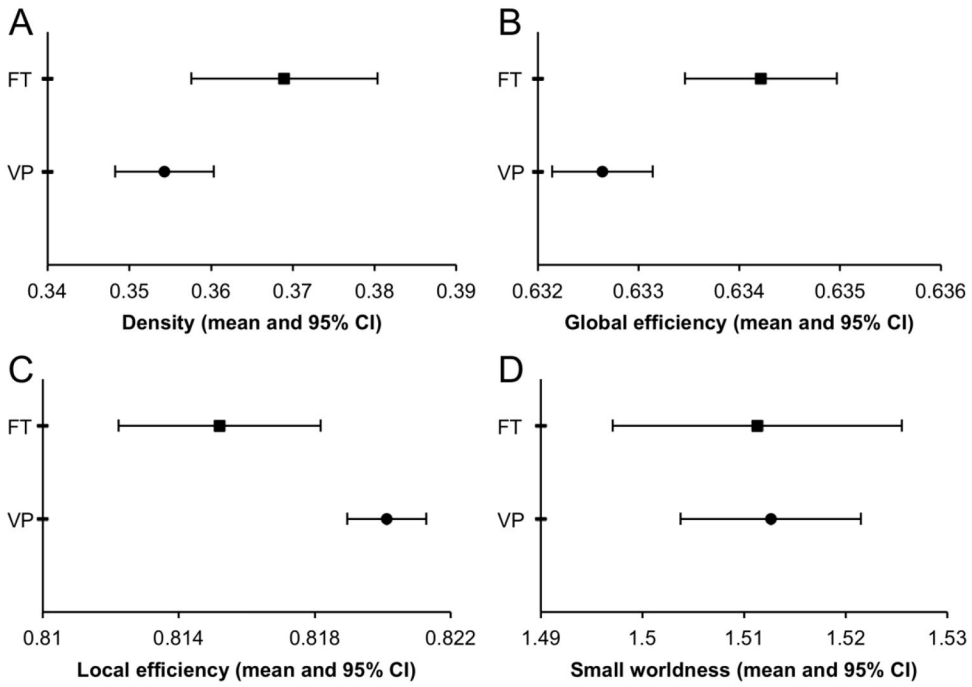

Fig. 1. Comparison of whole brain network measures between very preterm (VP) and full-term (FT) children at age 7 years: (A) Density, (B) Global efficiency, (C) Local efficiency, (D) Small worldness

Graphs show means and 95% confidence intervals (CI), adjusted for age at scan and intracranial volume.

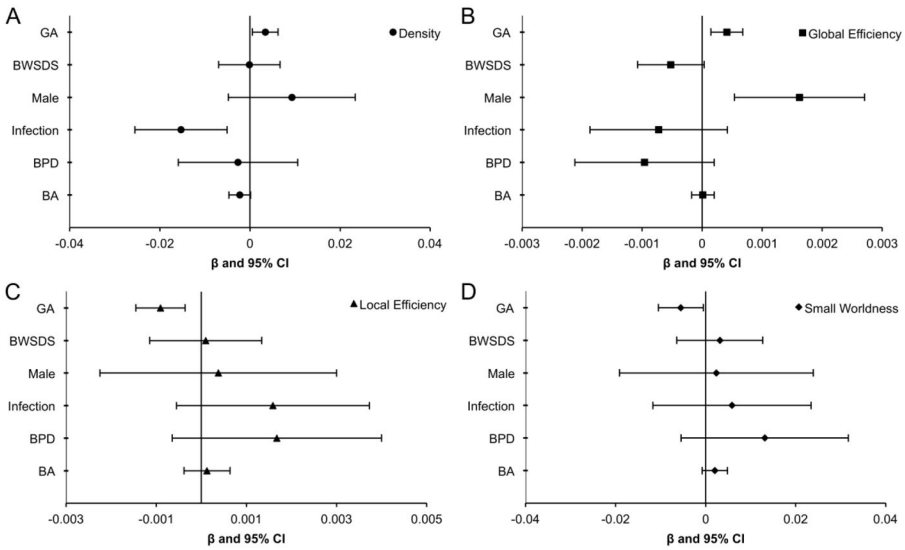

Fig 2. Perinatal predictors of whole brain network measures for very preterm children

Perinatal predictors of whole brain network measures for very preterm children for (A) Density, (B) Global efficiency, (C) Local efficiency and (D) Small-worldness. Graphs show regression coefficients (β) and 95% confidence intervals (CI) adjusted for age at scan and intracranial volume. β indicates the amount of change in the dependent variable for each unit change in the independent variable. Note results are not comparable across perinatal predictors and outcomes due to the different scales of both the predictors and the outcomes. GA = gestational age (weeks), BWSDS = birthweight standard deviation score, BPD = bronchopulmonary dysplasia, BA = brain abnormality.

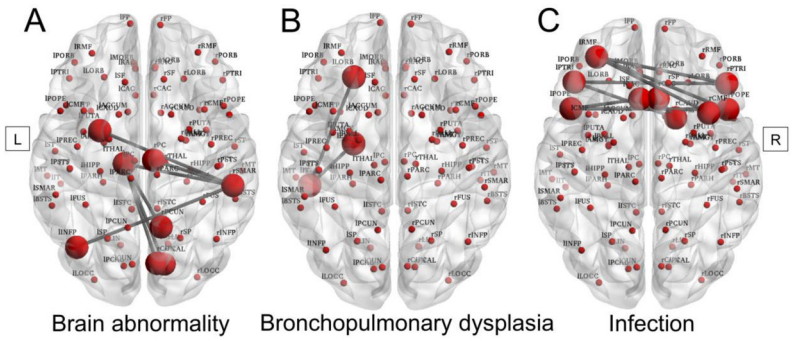

Fig 3. Connectivity sub-networks and perinatal predictors in very preterm children

Connectivity sub-networks illustrating connected nodes with reduced edge strength in very preterm children at 7 years of age associated with (A) qualitative brain abnormality, (B) bronchopulmonary dysplasia, and (C) infection at term-equivalent age. L= left, R= right.

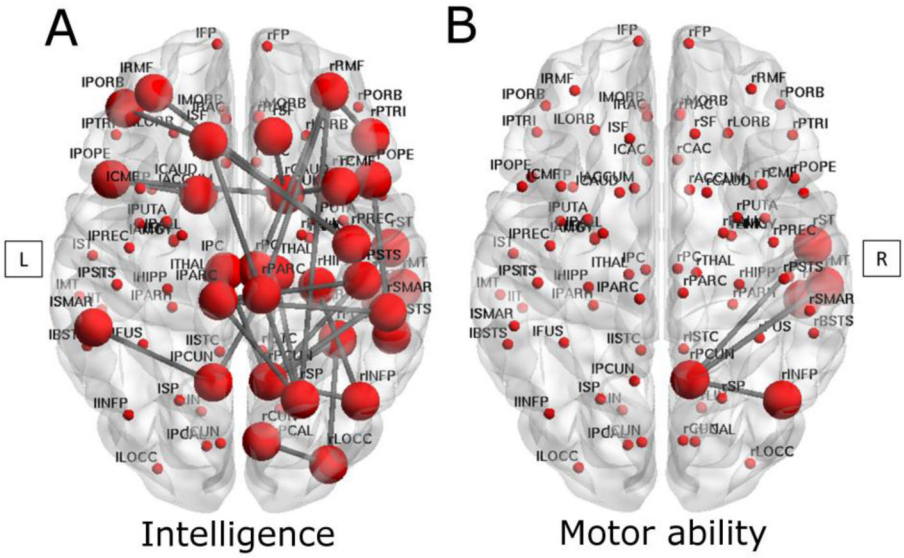

Fig 4. Connectivity sub-networks and neurodevelopmental impairment in very preterm children

Impaired intelligence (A) or impaired motor ability (B) associated with sub-networks of reduced edge strength between connected nodes in very preterm children at 7 years of age. L= left, R= right.

Table 1

Perinatal characteristics and 7 year outcomes for the very preterm (VP) and full-term (FT) groups

Perinatal characteristics	**VP, n=107**	**FT, n=26**	**Mean difference (95% CI)**
GA at birth (weeks), mean (SD)	27.4 (1.8)	38.8 (1.3)	−11.4 (−12.1, −10.6)
Birth weight (g), mean (SD)	970 (215)	3195 (512)	−2225 (−2353, −2097)
Birth weight SD score[a], mean (SD)	−0.5 (0.9)	−0.06 (1.0)	−0.4 (−0.8, −0.02)
			Difference in proportion (95% CI)
Male, n (%)	46 (43.0)	12 (46.2)	−0.03 (−0.24, 0.18)
Singleton, n (%)	53 (49.5)	24 (92.3)	−0.43 (−0.57, −0.28)
Small for GA[b], n (%)	9 (8.4)	1 (3.8)	0.05 (−0.05, 0.14)
Antenatal corticosteroids, n (%)	91 (85.8)[c]	0 (0)	0.86 (0.80, 0.92)
Postnatal corticosteroids[d], n (%)	4 (3.7)	0 (0)	0.037 (0.001, 0.073)
Sepsis, n (%)	31 (29.0)	1 (3.8)	0.25 (0.14, 0.36)
Necrotising enterocolitis, n (%)	6 (5.6)	0 (0)	0.06 (0.01, 0.10)
Infection[e], n (%)	34 (31.8)	1 (3.8)	0.28 (0.16, 0.39)
Bronchopulmonary dysplasia, n (%)	33 (30.8)	0 (0)	0.31 (0.22, 0.40)
Intraventricular haemorrhage grade III/IV, n (%)	1 (0.9)	0 (0)	0.009 (−0.009, 0.028)
Cystic periventricular leukomalacia, n (%)	3 (2.8)	0 (0)	0.028 (−0.003, 0.059)
			Median difference (95% CI)
Brain abnormality score, median (25^{th}–75^{th} percentile)	5 (3–7)[c]	1.5 (1–2)	3.0 (1.5, 4.5)
7-year characteristics			**Mean difference (95% CI)**
Age at scan (years), mean (SD)	7.5 (0.3)	7.6 (0.2)	−0.07 (0.17, 0.04)
Total intracranial volume (cm^3), mean (SD)	1326 (120)	1430 (105)	−104 (−155, −53)
Age at assessment (years), mean (SD)	7.5 (0.3)	7.6 (0.2)	−0.07 (−0.17, 0.03)
			Difference in proportions (95% CI)
Impaired intelligence [k], n (%)	10 (9.3)	1 (3.8)	0.05 (−0.04, 0.15)
Impaired reading [k], n (%)	18 (17.0)[c]	2 (7.6)	0.09 (−0.03, 0.22)
Impaired mathematics [k], n (%)	36 (34.0)[c]	4 (15.4)	0.19 (0.02, 0.35)
Impaired attention [k], n (%)	44 (42.7)[f]	6 (23.1)	0.20 (0.01, 0.38)
Impaired working memory [k], n (%)	50 (48.5)[f]	3 (12.0)[g]	0.37 (0.21, 0.53)
Impaired language [k], n (%)	21 (20.0)[h]	1 (4.0)[g]	0.16 (0.05, 0.27)
Impaired visual perception [k], n (%)	23 (23.0)[i]	2 (8.0)[g]	0.15 (0.02, 0.28)
Impaired motor ability [k], n (%)	13 (12.7)[j]	2 (7.7)	0.05 (−0.07, 0.17)

CI= confidence interval, GA = gestational age, SD= standard deviation.

[a]Computed relative to the British Growth Reference data (Cole et al. 998).

[b]birth weight SD score > 2 SD below mean weight for GA.

[c]n=106.

[d] Postnatal dexamethasone, usual dose 0.15 mg/kg per day for 3 days, reducing over 10 days: total dose 0.89 mg/kg.

[e] Proven sepsis and/or proven necrotising enterocolitis.

[f] n=103.

[g] n=25.

[h] n=105.

[i] n=100.

[j] n=102.

[k] Impairment was defined as scores more than 1 SD below the normative mean.